Materials Advances

ROYAL SOCIETY OF CHEMISTRY

PAPER

View Article Online
View Journal | View Issue

Cite this: *Mater. Adv.*, 2026, 7, 4128

Solvent-free 3D printing of silicone elastomers by digital light processing using an oligosiloxanyl substituted bis(acyl)phosphane oxide as photoinitiator

Debora Eiler,[a] Enzo Brack,[a] Yulia Yuts,[a] Desirée Baruffaldi,[b] Francesca Frascella,[b] Andrea Cosola,[b] Xun Sun,[c] Annalisa Chiappone,*[d] Yinyin Bao*[c] and Hansjörg Grützmacher*[ae]

Received 26th October 2025,
Accepted 19th March 2026

DOI: 10.1039/d5ma01233c

rsc.li/materials-advances

Silicone elastomers possess a wide range of advanced applications, particularly in biomedicine, soft robotics, and wearable electronics. Consequently, the fabrication of sophisticated 3D structures based on poly(dimethylsiloxane) (PDMS) formulations is essential to fully realize these applications. Light-based additive manufacturing methods such as digital light processing (DLP) offer the combination of favourable mechanical performance and high printing precision required for next-generation 3D-printed silicone elastomers. However, despite significant progress in this field, the development of a photoinitiating system compatible with PDMS formulations has been largely overlooked. In this work, we report a new photoinitiator, BAPO-SIL, and demonstrate its application in solvent-free 3D printing of silicone elastomers *via* DLP. BAPO-SIL exhibits excellent miscibility with a variety of PDMS polymer precursors such as TEGORad 2800 and novel norbornene derivatives, enabling straightforward resin formulation without the need for solvents or mechanical homogenization. Using BAPO-SIL, both commercially available PDMS acrylates and state-of-the-art thiol–norbornene PDMS resins were successfully 3D printed with high spatial resolution, showing good cytocompatibility by preliminary cell tests. Notably, the thiol–norbornene systems enabled the fabrication of ultrasoft silicone elastomers with a Young's modulus as low as 0.06 MPa and elongation at break up to 166%, highlighting the potential of BAPO-SIL for advanced silicone 3D printing applications.

Introduction

Silicone elastomers, polymer networks formed by crosslinking of poly(dimethylsiloxane) (PDMS), are extensively used in various industries due to their inertness, non-toxicity, and superior thermal stability.[1,2] These excellent properties are further amplified by their high transparency and biocompatibility, coupled with flexibility in material design. These capabilities have led to the widespread adoption of PDMS elastomers in diverse advanced applications, notably in the field of biomedicine, including medical implants,[3,4] microfluidic devices,[5,6] wearable electronics,[7,8] soft robotics,[9,10] and drug delivery.[11,12] As the complexity of applications for silicone elastomers grows, particularly in emergent research areas, the need for precise, sophisticated 3D structures becomes even more critical.

Current manufacturing techniques, such as soft lithography, are reliable but are labour-intensive and limited to two-dimensional layering, which restricts the three-dimensional intricacy of achievable structures.[13–15] Modern advancements in 3D printing technology, especially the innovative use of stereolithography (SLA)[16,17] and digital light processing (DLP),[18,19] are paving the way for the rapid production of durable and flexible silicone elastomers.[13,14,20–23] These vat photopolymerization-based techniques usually exploit radical photo-crosslinking reactions between acrylate monomers or thiol–ene reactions, differing from the extrusion based 3D printing techniques, such as direct ink writing (DIW).[24] In this perspective, PDMS-like materials have been functionalized with acrylate or vinyl groups, able to react with thiol groups making polysiloxanes suitable for vat

[a] *ETH Zürich, Department of Chemistry and Applied Biosciences, Vladimir-Prlog Weg 1, 8093 Zürich, Switzerland. E-mail: hgruetzmacher@ethz.c*
[b] *Politecnico di Torino, Department of Applied Science and Technology, Corso Duca degli Abruzzi, 24, 10129, Torino, Italy*
[c] *University of Helsinki, Department of Chemistry, PL 55 (A. I. Virtasen aukio 1), 00014 Helsinki, Finland. E-mail: yinyin.bao@helsinki.fi*
[d] *University of Cagliari, Chemical Science and Geology Department, DSCG, Cittadella Universitaria (Blocco D), S.S. 554 bivio per Sestu, 09042, Monserrato (CA), Italy. E-mail: annalisa.chiappone@unica.it*
[e] *LIFM, IGCME, School of Chemistry, Sun Yat-Sen University, 510006 Guangzhou, China*

printing and promising to transcend the limitations of traditional molding methods. In addition, nanoparticles[13] or microparticles[23] can be added to the resin formulation in order to further streamline tailor-made fabrication of silicone elastomers. This approach merges enhanced mechanical properties with the high precision required for the next generation 3D printed silicone elastomers.

Among these systems, an often-overlooked issue is the use of photoinitiators, which are in general solids and therefore poorly soluble and compatible with the PDMS formulations. In general, there are two ways of mixing the photoinitiators with PDMS formulations: using homogenizer/ball mill or using organic solvents. The homogenizing method is usually a multi-step process, tedious and time-consuming, with a certain risk of premature-crosslinking.[13,23–25] On the other hand, using organic solvents (*e.g.*, dichloromethane or toluene) to dissolve the photoinitiators for resin formulation requires removing the solvents before or after the printing process, which generates unnecessary waste.[20,25] Furthermore, post-printing removal of solvents can cause a shrinkage of the final 3D printed object.[26]

Specifically, the commercially available bisacylphosphane oxide (BAPO) $PhPO(COMes)_2$ (Omnicure 819) is a crystalline solid with very limited solubility, leading to suboptimal compatibility with 3D printing polymers. Nonetheless, modification of this photoinitiator can enhance its compatibility with photopolymers.[27,28] We have shown that BAPO groups can be grafted onto polyethylene glycol (PEG),[29] poly(amidoamine) and gelatin,[30] γ-cyclodextrin,[31,32] and even cellulose nanocrystals[33] to facilitate their efficiency and the compatibility with the materials used for 3D printing. Recently, BAPO-modified polyesters were synthesized by ring-opening polymerization of D,L-lactide and ε-caprolactone initiated by hydroxyl BAPO molecules. This polymerization transformed solid BAPO molecules to liquid macrophotoinitiators,[26] facilitating solvent-free 3D printing of biodegradable elastomers.[34,35] Liquid initiators based on BAPOs carrying branched alkyl chains were also used for the DLP 3D printing of PDMS-like microfluid devices, showing however some limits of solubility.[35] A BAPO initiator was also used in a mixture with liquid 2-hydroxy-2 methylpropiophenone as solvent in presence of a second initiator to boost the reactivity of silicon acrylate formulations.[36] To further improve BAPO's compatibility with PDMS, we envisaged that BAPO molecules could be combined directly with polysiloxane moieties to render them liquid and make them sufficiently miscible in frequently applied siloxane formulations. Note in this context that the liquid photoinitiator ethyl (2,4,6-trimethylbenzoyl)phenylphosphinate (TPO-L) has already been employed in the SLA printing of silicone elastomers, in this case, isopropyl-thioxanthone (ITX) was used as co-initiator to give an optimized formulation (0.6% TPO-L and 0.3% ITX) with the need of THF as solvent.[14]

Here, we present a new photoinitiator, BAPO-SIL, and its application for solvent-free 3D printing of silicone elastomers by DLP. The photoinitiator shows high miscibility with various PDMS polymer precursors, enabling convenient resin formulation without using solvents or homogenizers. Using BAPO-SIL, commercially available PDMS acrylates and state-of-the-art thiol–norbornene PDMS resins have been both successfully 3D printed with high resolution. According to preliminary tests, the obtained materials showed that the typical cytocompatibility of PDMS is maintained using the new initiator. Moreover, the thiol-norbornene resins enabled the fabrication of ultrasoft silicone elastomers with good stretchability.

Results and discussion

Synthesis and characterization of BAPO-SIL

A very efficient way for the preparation of bis(acyl)phosphane oxides, BAPOs, is the addition of bis(acyl)phosphane $HP(COMes)_2$ (BAPH) to acrylate functions (Phospha-Michael-addition) followed by oxygenation with a peroxide such as hydrogenperoxide, H_2O_2, or *tert.*-butylhydroperoxide, *t*BuOOH.[38] In a first attempt, we therefore sought to prepare oligo- or polymeric siloxanes with pending acrylate functions, which may also act as multiple-photoinitiators.[32] To achieve this, we first followed standard procedures in which commercially available $Me_2Si(OMe)_2$ was co-condensed with $Me(MeO)_2Si–(CH_2)_3–O–CO–CH{=}CH_2$ [3-(dimethoxy(methyl)silyl)propyl acrylate] in acetic acid.[39] According to mass spectrometric analysis this led to a mixture of cyclo(siloxanes) with ring sizes between 8–12 (D_4, D_5, D_6) and only partial incorporation of the acrylate substituted siloxy unit (ratio of Me_2SiO to $Me[H_2C{=}CH–CO_2(CH_2)_3]SiO$ units ≈9 : 1; av. molecular weight, M_n = 820 g mol^{-1}). When this mixture was reacted with $HP(COMes)_2$ (**BAPH**) in the presence of 10 mol% tetramethylguanidine (TMG) as catalyst, addition of the $P(COMes)_2$ (BAP) unit to the acrylate was observed but resulted in an inseparable mixture of compounds. In another approach, we therefore added **BAPH** first to 3-(dimethoxy(methyl)silyl)-propyl acrylate, which after oxidation with *tert.*butylhydroperoxide, *t*BuOOH, cleanly gave the desired BAPO-SIL compound $Me(MeO)_2Si–(CH_2)_3–O–CO–(CH_2)_2–PO(COMes)_2$ (**1a**) in almost quantitative yield (>96%) (Scheme 1).

However, co-condensation of this compound with $Me_2Si(OMe)_2$ under various conditions using acetic acid or HCl as catalyst in solvents such as EtOH or toluene gave again mixtures of oligo- and polysiloxanes (M_n 1840–2700 g mol^{-1}) with very large polydispersion indices, PDIs, of up to 9. On top of this, some of the compounds prepared that way were insoluble in organic solvents or siloxane formulations. We therefore abandoned the idea of preparing a defined BAPO substituted oligo/polysiloxane by one of these polycondensation methods. But the excellent yield in the synthesis **1a**, which itself however is insoluble in siloxane formulations, prompted us to react **BAPH** with a commercially available polysiloxane-methacrylate with a molecular weight of about ∼600 g mol^{-1} [that is X_{av} = 4.4 in $Bu(Me_2)Si–O(Me_2SiO)_x–Me_2Si–(CH_2)_3–O–CO–CH(CH_3){=}CH_2$] in the hope that this will lead to a photoinitiator soluble in siloxane formulations. The Phospha-Michael addition proceeded again smoothly in dry DME as solvent in the presence of 10 mol% TMG. Because of the steric hindrance caused by the methyl group attached to the acrylate function the reaction

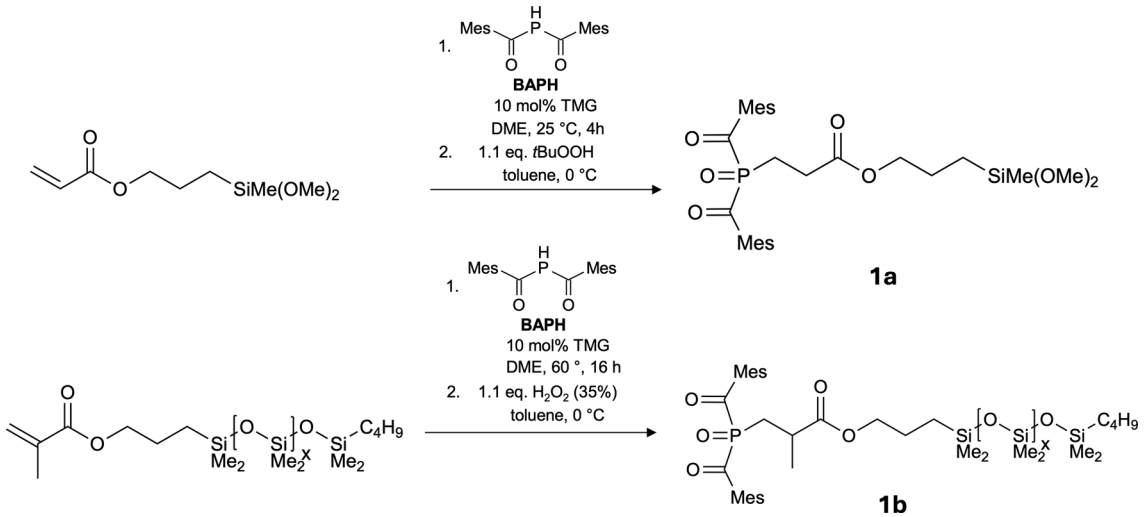

Scheme 1 Synthesis of the two BAPO-SIL compounds **1a** (>96%) and **1b** (90%).

temperature needs to be raised to 60 °C. After evaporation of all volatiles, the crude product remaining in the reaction vessel is dissolved in toluene and oxygenated with 35% H_2O_2 to give the final product **1b** as viscous yellow oil again in excellent yield (90%). As will be shown below, compound **1b** shows good to excellent miscibility with most siloxane acrylates commonly employed industrially.

3D printing of silicone elastomers from PDMS acrylate resins

At first, the suitability of BAPO-SIL for the polymerization of commercial silicone acrylate monomers was checked by mixing 1 wt% of the liquid initiator with five monomers, which are commercially available (information on the molecular structure of these monomers is given in the Supporting Information). The miscibility of BAPO-SIL **1b** with these monomers was visually evaluated (see SI) and we find that with four monomers completely transparent formulations are obtained while only one resulted in a slightly opaque mixture. Nevertheless, according to photorheology tests, all formulations are photoactive and after short irradiation times (see SI) promising preliminary results were obtained.

TEGORad 2800 was then selected to perform an in-depth investigation on the reactivity and printability using BAPO-SIL **1b** as photoinitiator. This polymer was selected as a benchmark, being known its suitability for 3D printing[36] as well as its cytocompatibility in the presence of other initiators.[37]

The first tests aimed at evaluating the reactivity and printability using a DLP apparatus with a light source in the UV range (380 nm) and relatively high light intensity. The photorheology tests (Fig. 1a) performed using a light source that mimics the 3D printer, showed that the TEGORad 2800 monomer rapidly gives crosslinked polymers using BAPO-SIL as initiator. Indeed the G' value increases by about five orders of magnitude in few seconds and reaches its plateau in 15 seconds. Furthermore, two concentrations of initiator were tested *i.e.* 1 wt% and 0.1 wt% showing that BAPO-SIL **1b** can impart high reactivity even when used in low amounts. Indeed, the increase of the G' modulus of the sample containing 0.1 wt% of photoinitiator (Fig. 1b) shows a delay in the first seconds of irradiation in comparison to formulations with a higher content of **1b** maintaining, nevertheless, a good reactivity with the increase of the G' value of several orders of magnitude within the first 12 seconds.

The kinetics of photopolymerization of TEGORad 2800 using BAPO-SIL as a photoinitiator were also compared with those obtained using the commercial photoinitiator TPO-L (Fig. 1a and b). TPO-L, a liquid photoinitiator that is also miscible with silicone-based monomers, was used without co-initiators at twice the molar concentration of BAPO-SIL to ensure that both formulations contained equimolar amounts of radical-generating photoactive groups. Under these conditions, similar activity was observed at high concentrations. However, at lower concentrations, BAPO-SIL exhibited superior performance compared with TPO-L, demonstrating the greater suitability of the silicone-based initiator for silicone photocuring.

The data obtained from photorheology tests indicate that the investigated formulations are suitable for 3D printing. Thus, different tests were performed and the printing parameters were optimized. Fig. 1b and c display objects with complex geometries printed using 1 wt% of initiator adjusting the layer thickness at 100 μm and the exposure time at 6 s. The objects present millimetric features and precise details. Slight over-polymerization in the x–y plane in the first layer region is observed due to longer exposure times needed in this range; this can eventually be resolved with the use of a dye. When a lower amount of initiator was used, complex 3D structures were hard to obtain despite an increase in printing time (12 s). Nevertheless, it has been possible to obtain 2.5 D designs, good for microfluidic channels (channel dimension 1 mm).

The crosslinked polymers prepared with the higher amount of PI (*i.e.* 1 wt% BAPO Sil and double molar amount of TPO-L) were characterized in terms of mechanical properties. Dumbbell specimens were printed and subjected to tensile test (Fig. 2e and f). The results indicated similar elastic moduli

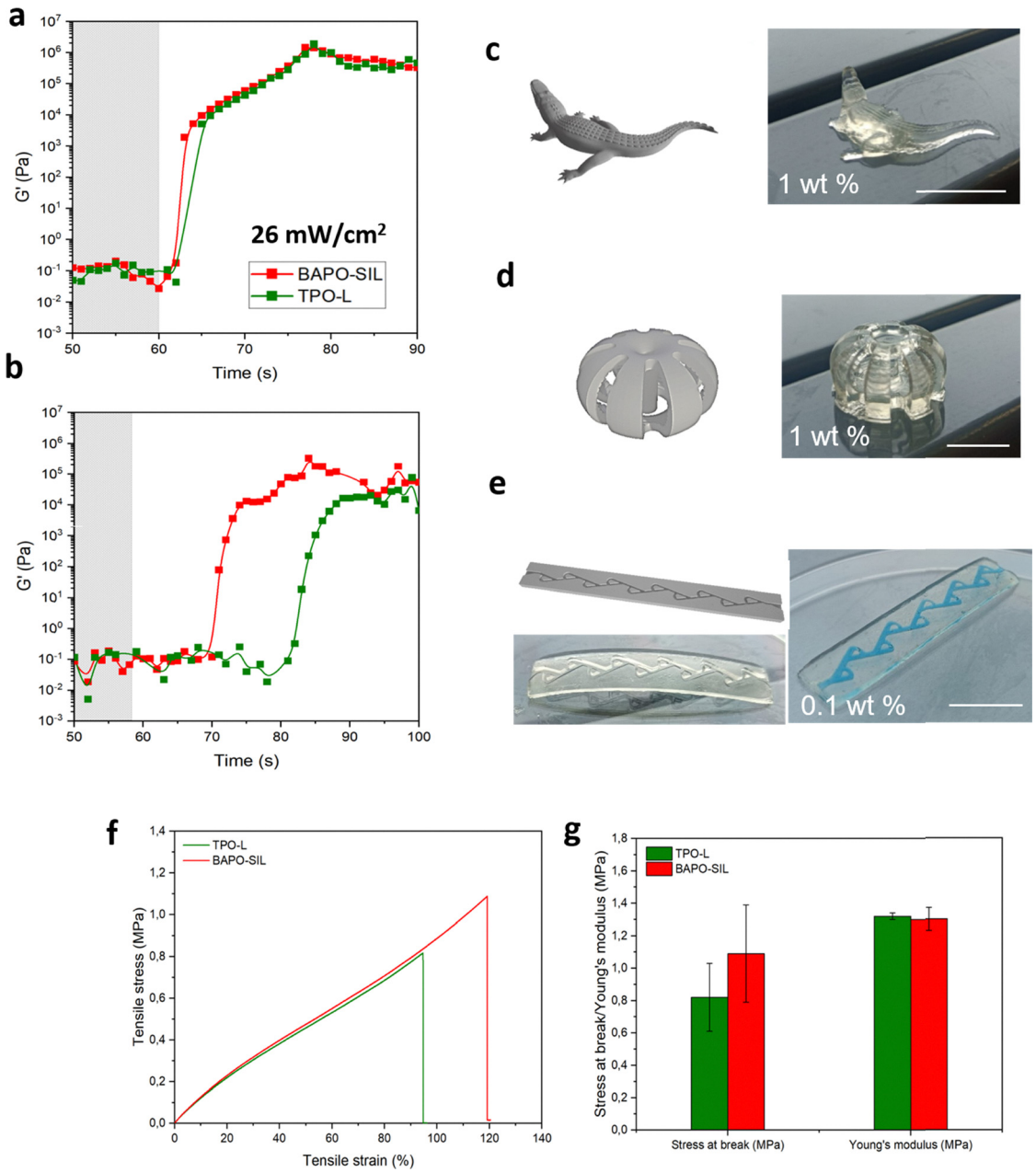

Fig. 1 Photo-rheology curves showing the photopolymerization kinetics of TEGOrad 2800 using BAPO-SIL (1 wt% and 0.1 wt%, Figures a and b, respectively) or TPO-L as photoinitiator. TPO-L was used at twice the molar concentration of BAPO-SIL to ensure that the final formulations contained equimolar amounts of photoactive groups. A UV-vis broad emission lamp (intensity: 26 mW cm^{-2}) was used as the light source. (c), (d) 3D Models and objects printed using a UV printer in TEGORad using 1 wt% of BAPO-SIL. (e) Fluidic channel printed in TEGORad using 0.1 wt% of BAPO-SIL: the right image shows the channel filled with blue colored water. (f), (g) Tensile test performed on the 3D-printed TEGORad specimens evaluated using dumbbell-shaped samples conforming to ASTM D638 Type IV standards. Two formulations were tested: one with 1% w/w BAPO-SIL and the other with TPO-L at twice the molar concentration of BAPO-SIL.

for both samples, consistent with values reported in the literature for the same monomer.[36] The average stress at break was slightly higher for the sample prepared with BAPO-SIL; however, the difference falls in the range of experimental error. These data suggest that the different photoinitiators do not significantly affect the mechanical performance of the PDMS elastomer. Similarly, the specimen exhibited comparable mechanical performance under cyclic test conditions (See SI Fig. S2). Negligible hysteresis was observed over the ten loading–unloading cycles, except for a slight energy dissipation in the first cycle that was not recovered in subsequent ones. These findings underline that the macroscopic characteristics of the cured material are not affected by the nature of the photoinitiator, indicating that BAPO-SIL can be used as an alternative photoinitiator for the 3D printing of silicone elastomers, ensuring high crosslinking density and rapid reactivity even at low concentrations.

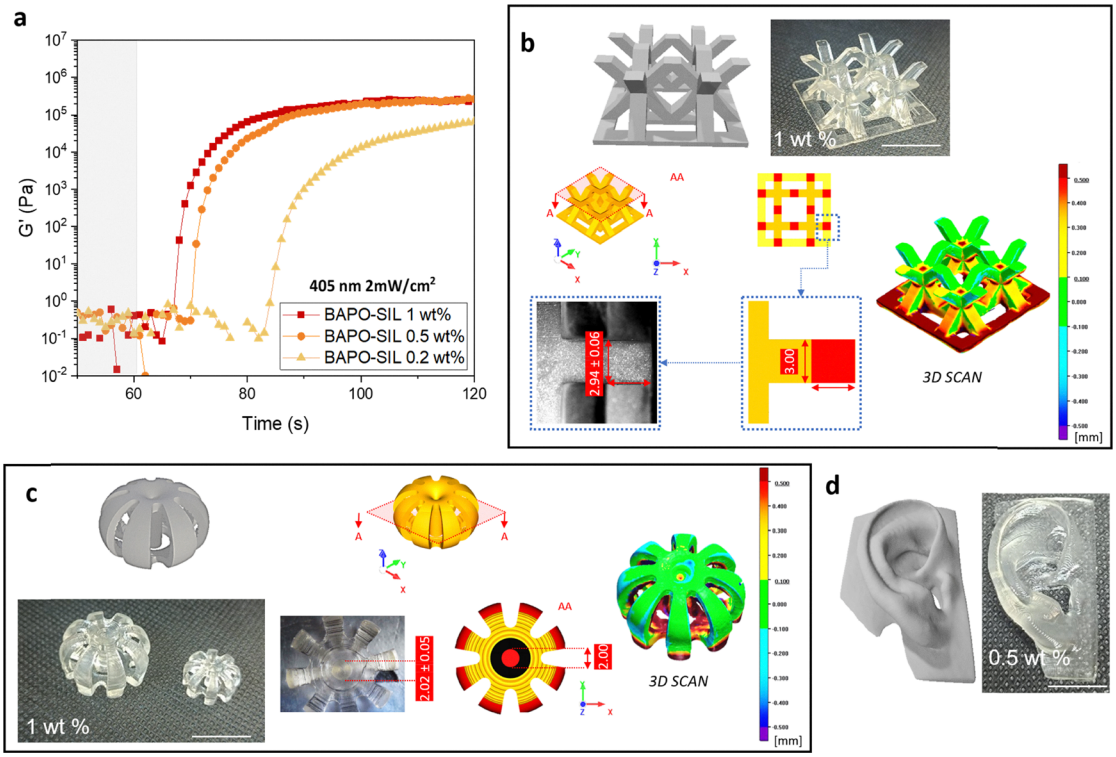

Fig. 2 (a) Photorheology plots for TEGORad monomer in presence of 1 and 0.5 wt% and 0.2 wt% of BAPO-SIL **1b** performed using a LED light source @405 nm, light intensity 2 mW cm^{-2}. (b), (c) 3D Models and objects printed using a LCD printer @405nm in TEGORad using 1 wt% of BAPO-SIL **1b** and evaluation of their printing fidelity by optical microscope measurements and 3D scan. (d) Human ear model printed in TEGORad using 0.5 wt% of BAPO-SIL **1b**.

In order to assess the capability of BAPO-SIL to be used as initiator in formulations on different commercial printers, a stereolithographic device based on an LCD with visible light emission and low light intensity was used.

The reactivity of the monomer in the presence of different amounts of BAPO-SIL **1b** was again tested by photorheology mimicking the conditions eventually used in a printing process (irradiation 405 nm, 2 mW cm^{-2}). As visible from Fig. 2a, the kinetics of polymerization is slowed down – as to be expected – due to the lower energy input. However, the formulations still maintain good reactivity when the initiator concentration is above 0.5 wt%. The curves of the formulations containing 1 wt% and 0.5 wt% of **1b** present a delay of 7 and 11 s respectively before the increase of the G′ value, that, nevertheless reaches its maximum within 25 s of irradiation. It is important to note that the final value reached by G′ corresponds to the one observed in the previous experiment ($>10^5$ Pa) and is in line with previous studies.[36] The observed behaviour indicates that these formulations are still suitable for VAT printing under the applied conditions. Using a lower amount of PI, however, leads to a highly delayed polymerization and the final modulus is reduced, indicating the incomplete crosslinking of the network. Consequently, printing processes with low amounts of **1b** are only suitable for standard polymerization processes that can be performed with longer exposure times but these conditions are not applicable for VAT printing with low light intensity.

As a further proof of concept, two formulations containing 1 and 0.5 wt% of **1b** were 3D printed using an LCD printer. By setting a layer thickness of 50 μm and a layer exposure time of 12 s, it was possible to produce precise objects with millimetric features when using the highest amount of **1b** (Fig. 2b and c). The printing resolution of these objects was evaluated by comparing the dimension of the printed object with those of the original CAD model. The analysis was performed both by collecting images using an optical microscope and by conducting a 3D scan of the printed objects. The results of the comparative analysis indicate that the deviation between positive and negative displacements of the 3D-printed parts relative to the CAD model was ±0.06 mm, in good agreement with the values observed *via* optical microscopy (±0.05 mm). Reducing the content of PI to 0.5 wt% while increasing the exposure time even to 20 s, it was not possible to obtain the same precision features as before (Fig. 2d) but it has been possible to print larger objects with less complex features (Fig. 2e).

These preliminary tests demonstrate that the new initiator BAPO-SIL is an excellent candidate for compounding of formulations suitable for VAT printing of silicone-based materials. The initiator is easily miscible with commercial silicon-acrylate monomers and ensures high reactivity even at low concentrations, without the use of solvents or co-initiators.

3D printing of silicone elastomers from thiol–norbornene PDMS resins

In order to make another step forward in the development of silicone-based formulations suitable for photopolymerisations,

the suitability of BAPO-SIL for the 3D printing of innovative monomers was also assessed. Thiol–ene reactions in particular thiol-norbornene reactions attract more and more attention in the field of light-based 3D printing due to the fast polymerization rate, and the high tolerance to oxygen inhibition.[40–42] To evaluate the printability of thiol-norbornene PDMS resins using our BAPO-SIL photoinitiator, we formulated PDMS-SH and PDMS-NB (93/7, w/w) at different concentrations of BAPO-SIL, and tested the curing depth under different light exposure times.[26,43] As shown in Fig. 3, 1.5 wt% BAPO-SIL was used first for the formulation, which provided very high curing depth, about 700 μm at 4 s of exposure time. To reduce the penetration depth, Sudan I was added to the resin as a light absorber. However, significant curing depth was still observed with >400 μm at 2 s of exposure time. The high penetration can be also reflected from the resolution test as shown in Fig. 3b. Eventually, we reduced the concentration of BAPO-SIL to 0.75 wt%, and proper light penetration can be obtained with curing depth of about 200 μm at 2 s of exposure time. The printed strips show good resolution with smooth surfaces (Fig. 3b). We therefore further selected this composition of the formulation for the following 3D printing tests.

To evaluate the mechanical properties of the 3D printed PDMS networks, we printed dog-bone shape specimens (Fig. 4a, inset) from two formulations with PDMS-SH and PDMS-NB in a ratio of 93/7 and 86.5/13.5 (w/w), respectively. As shown in Fig. 4a, both specimens show good elasticity with average elongation at break of 147% and 166%, respectively. The Young's modulus was determined to be 0.17 MPa for the 93/7 while the value for the 86.5/13.5 formulation was only 0.06 MPa, indicating

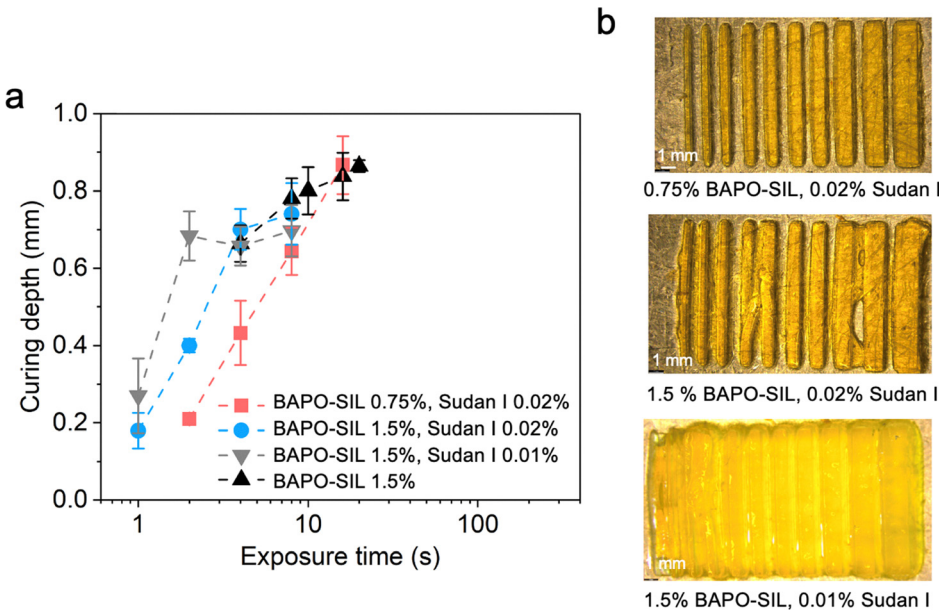

Fig. 3 (a) Log–linear plot of the cure depth *versus* exposure time for different concentrations of BAPO-SIL **1b** and Sudan I ($n \geq 3$). The slopes of the lines determine the characteristic penetration depth of the resins. (b) Resolution test based on the different formulations.

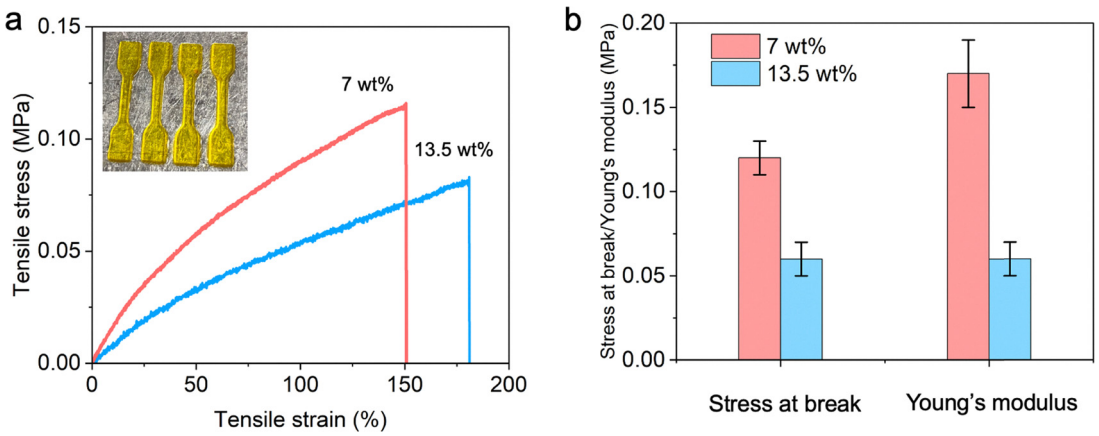

Fig. 4 (a) Stress–strain curves obtained from the tensile test based on two formulations with 7 wt% and 13.5 wt% of PDMS-SH. Inset: 3D printed dog-bone shape specimens; (b) the corresponding stress at break and Young's modulus obtained ($n \geq 3$).

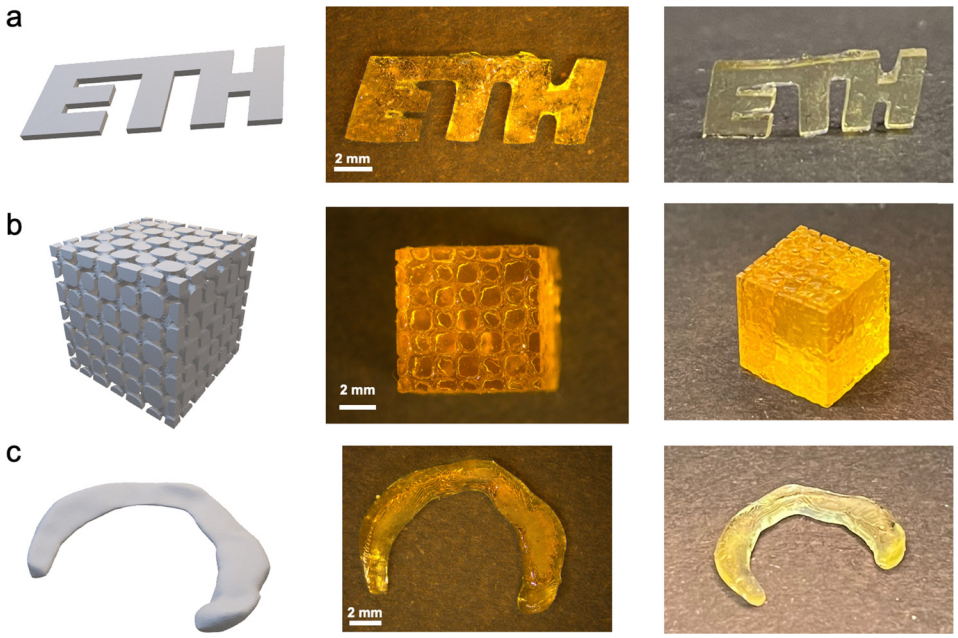

Fig. 5 Digital design and photographs of the (a) 3D printed ETH logo, (b) a cube with a rough surface, and (c) a meniscus model from PDMS-SH and PDMS-NB (93/7, w/w) with 0.75 wt% BAPO-SIL **1b**.

the highly soft nature of the PDMS elastomer with lower cross-linking density. Accordingly, the maximum stress of the elastomers was determined to be significantly lower at 0.12 and 0.06 MPa, respectively (Fig. 4b). These "super-soft" PDMS elastomers could be interesting materials to be applied in the fields of soft robotics, bioelectronics and medical devices.[44–46]

With the excellent mechanical properties obtained, we further evaluated the printability of complex structures of the thiol-norbornene PDMS materials using BAPO-SIL **1b**. The ETH logo and a cube with a rough surface were successfully printed using the PDMS-SH and PDMS-NB formulations (93/7, w/w) with 0.75 wt% **1b** (Fig. 5a and b) despite the highly soft properties. The surface feature of the cube can be clearly visualized. The overcured part of the ETH logo is due to the longer exposure time for the bottom layer, which does not appear in the rest of the layers. Subsequently we applied the same formulation for DLP printing of a model of a meniscus, and the structure can be well fabricated with a smooth surface and high fidelity (Fig. 5c). In combination these results demonstrate the good printability of the PDMS resin with BAPO-SIL **1b** as photoinitiator, indicating its potential as component for resins in soft silicone material manufacturing.

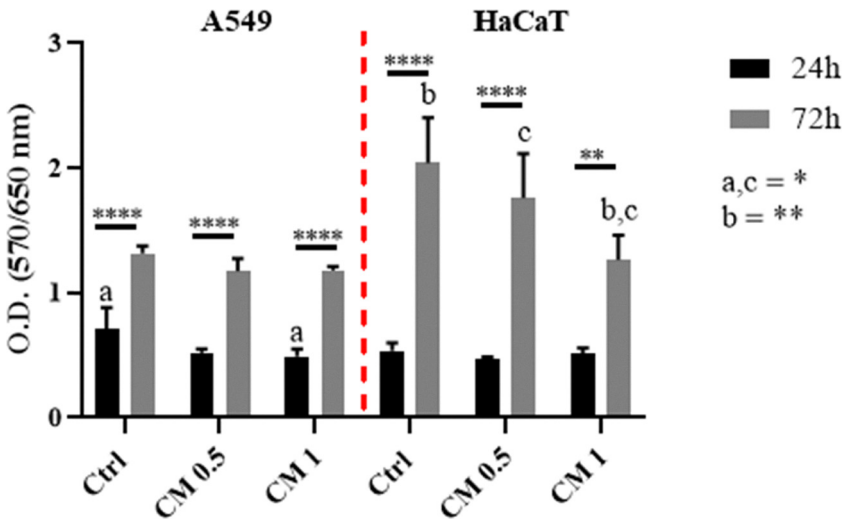

Fig. 6 MTT assay on A549 or HaCaT incubated with normal medium (Ctrl) or conditioned ones (*i.e.* CM 0.5 and CM 1) after 24 or 72 h of culture. The results were shown as mean +/− standard deviation and the statistical analysis was carried out with two-way ANOVA tests where * = $p < 0.05$, ** = $p < 0.01$ and **** = $p < 0.0001$.

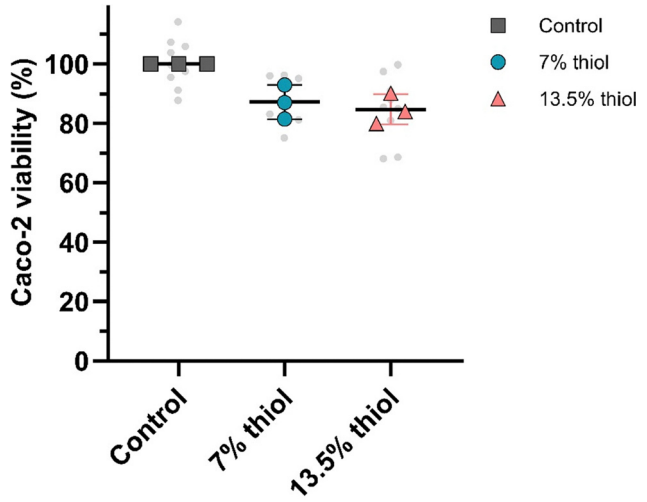

Fig. 7 Cytotoxicity profiles expressed as Caco-2 cell viability incubated with the extracts of 3D printed PDMS samples from thiol-norbornene resins with 7 wt% and 13.5 wt% PDMS-SH for 24 h.

Cytocompatibility of the printed silicon structures

The formulations investigated above were used to print platforms for the establishment of cell cultures. To assess the feasibility of its use for biological and medical applications, the release of cytotoxic compounds was assessed. Specifically, printed disks made of TEGORad with 0.5% or 1% of photoinitiator were incubated in a cell culture medium for 48 h, then the conditioned media (*i.e.* CM 0.5 and CM 1) were used to grow keratinocytes (*i.e.* HaCaT) and lung cancer cells (*i.e.* A549). As shown in Fig. 6 under all conditions applied in this work, cells maintained a high level of proliferation from 24 h to 72 h. Although HaCaT proliferation was slowed down by compounds released from the samples in which a higher amount of photoinitiator was used, over all the obtained results demonstrated the possibility to use the designed material as platforms for cell cultures.

Likewise, the cytotoxicity profile of the 3D printed PDMS materials using the thiol-norbornene resins was evaluated using the 3-(4,5-dimethylthiazol-2-yl)–5-(3-carboxymethoxyphenyl)–2-(4-sulfophenyl)–2H-tetrazolium (MTS) assay on Caco-2 cells. As shown in Fig. 7, cells incubated with the extracts of the 3D printed samples remained viable for both formulations, with a cell viability exceeding 80%.

Conclusion

The problem of finding a highly efficient photoinitiator, which is easily miscible in oligo- or polysiloxy acrylate formulations thereby allowing their efficient radical polymerization at low concentrations, can be solved by synthesizing bis(acyl)phosphinoxides (BAPOs) carrying a sufficiently long siloxy tail at the phosphorus center. These molecules are easily accessible from the remarkably stable phosphine $HP(COMes)_2$ (BAPH) and commercially available siloxy acrylates *via* a Phospha-Michael addition in presence of an organo catalyst such as tetramethylguanidine followed by oxygenation using a peroxide. The new photoinitiator BAPO-SIL **1b** was investigated in detail for the photopolymerization and specifically the light induced 3D-printing of two different types of formulations. On one hand the more classical 3D printing of silicone elastomers from poly(dimethyl)-siloxy (PDMS) acrylate resins could be achieved. On the other, the less well-established photopolymerization of siloxy thiols, PDMS-SH, and siloxy norbornene derivatives, PDMS-NB, could be initiated. In both cases, excellent printability giving objects with high-resolution at relatively low photoinitiator concentration could be achieved. Preliminary toxicity tests show that the well-established low toxicity of silicone materials is not jeopardized by the use of BAPO-SIL. In combination, the results reported here using BAPH as building block for tailor-made siloxy BAPOs hold great potential for the further development of photolithographic processes for the synthesis of new silicone-based materials.

Conflicts of interest

There are no conflicts to declare.

Data availability

Here we confirm the data for ''Solvent-free 3D printing of silicone elastomers by digital light processing using an oligosiloxanyl substituted bis(acyl)phosphane oxide as photoinitiator'' including NMR, MS, GPC, rheology, mechanical tests, cell culture tests and other relevant data are available at ETH Zurich's repository ''Research Collection'' at [www.research-collection.ethz.ch], after the publication in *Materials Advances*.

Acknowledgements

Y. B. is grateful for the support of Prof. Jean-Christophe Leroux (ETH Zurich) and the financial support from University of Helsinki. H.G. acknowledges the support of the ETH Zürich and the Lehn Institute of Functional Materials (LIFM) at Sun Yat Sen University. A. C. acknowledges Fondazione di Sardegna, Convenzione Triennale tra la Fondazione di Sardegna e gli Atenei Sardi, Regione Sardegna, L.R. 7/2007, 2022, project VOC_3D ''3D printed optical VOC sensors for indoor air quality evaluation'' CUP F73C23001590007, for financial support.

References

1 P. Mazurek, S. Vudayagiri and A. L. Skov, How to tailor flexible silicone elastomers with mechanical integrity: a tutorial review, *Chem. Soc. Rev.*, 2019, **48**(6), 1448–1464, DOI: 10.1039/C8CS00963E.

2 L.-H. Cai, T. E. Kodger, R. E. Guerra, A. F. Pegoraro, M. Rubinstein and D. A. Weitz, Soft Poly(dimethylsiloxane) Elastomers from Architecture-Driven Entanglement Free Design, *Adv. Mater.*, 2015, **27**(35), 5132–5140, DOI: 10.1002/adma.201502771 (acccessed 2023/11/24).

3 C. T. K. Khoo, Silicone synovitis: The current role of silicone elastomer implants in joint reconstruction, *J. Hand Surg. Br. Eur. Vol.*, 1993, **18**(6), 679–686, DOI: 10.1016/0266-7681(93)90222-2.
4 J. P. Heggers, N. Kossovsky, R. W. Parsons, M. C. Robson, R. P. Pelley and T. J. Raine, Biocompatibility of Silicone Implants, *Ann. Plast. Surg.*, 1983, **11**(1), 38–45.
5 K. Raj M and S. Chakraborty, PDMS microfluidics: A mini review, *J. Appl. Polym. Sci.*, 2020, **137**(27), 48958, DOI: 10.1002/app.48958 (acccessed 2023/11/24).
6 T. Fujii, PDMS-based microfluidic devices for biomedical applications, *Microelectron. Eng.*, 2002, **61–62**, 907–914, DOI: 10.1016/S0167-9317(02)00494-X.
7 D. Qi, K. Zhang, G. Tian, B. Jiang and Y. Huang, Stretchable Electronics Based on PDMS Substrates, *Adv. Mater.*, 2021, **33**(6), 2003155, DOI: 10.1002/adma.202003155 (acccessed 2023/11/24).
8 S. H. Jeong, S. Zhang, K. Hjort, J. Hilborn and Z. Wu, PDMS-Based Elastomer Tuned Soft, Stretchable, and Sticky for Epidermal Electronics, *Adv. Mater.*, 2016, **28**(28), 5830–5836, DOI: 10.1002/adma.201505372 (acccessed 2023/11/24).
9 F. Ilievski, A. D. Mazzeo, R. F. Shepherd, X. Chen and G. M. Whitesides, Soft Robotics for Chemists, *Angew. Chem., Int. Ed.*, 2011, **50**(8), 1890–1895, DOI: 10.1002/anie.201006464 (acccessed 2023/11/24).
10 O. D. Yirmibesoglu, J. Morrow, S. Walker, W. Gosrich, R. Cañizares, H. Kim, U. Daalkhaijav, C. Fleming, C. Branyan and Y. Menguc, Direct 3D printing of silicone elastomer soft robots and their performance comparison with molded counterparts, *2018 IEEE International Conference on Soft Robotics (RoboSoft)*, 2018, 295–302, DOI: 10.1109/ROBOSOFT.2018.8404935.
11 J. Di, S. Yao, Y. Ye, Z. Cui, J. Yu, T. K. Ghosh, Y. Zhu and Z. Gu, Stretch-Triggered Drug Delivery from Wearable Elastomer Films Containing Therapeutic Depots, *ACS Nano*, 2015, **9**(9), 9407–9415, DOI: 10.1021/acsnano.5b03975.
12 K. Malcolm, D. Woolfson, J. Russell, P. Tallon, L. McAuley and D. Craig, Influence of silicone elastomer solubility and diffusivity on the in vitro release of drugs from intravaginal rings, *J. Controlled Release*, 2003, **90**(2), 217–225, DOI: 10.1016/S0168-3659(03)00178-0.
13 K. Wang, W. Pan, Z. Liu, T. J. Wallin, G. van Dover, S. Li, E. P. Giannelis, Y. Menguc and R. F. Shepherd, 3D Printing of Viscoelastic Suspensions via Digital Light Synthesis for Tough Nanoparticle–Elastomer Composites, *Adv. Mater.*, 2020, **32**(25), 2001646, DOI: 10.1002/adma.202001646 (acccessed 2023/11/24).
14 N. Bhattacharjee, C. Parra-Cabrera, Y. T. Kim, A. P. Kuo and A. Folch, Desktop-Stereolithography 3D-Printing of a Poly(dimethylsiloxane)-Based Material with Sylgard-184 Properties, *Adv. Mater.*, 2018, **30**(22), 1800001, DOI: 10.1002/adma.201800001 (acccessed 2023/11/24).
15 N. Bhattacharjee, A. Urrios, S. Kang and A. Folch, The upcoming 3D-printing revolution in microfluidics, *Lab Chip*, 2016, **16**(10), 1720–1742, DOI: 10.1039/C6LC00163G.
16 R. J. Mondschein, A. Kanitkar, C. B. Williams, S. S. Verbridge and T. E. Long, Polymer structure-property requirements for stereolithographic 3D printing of soft tissue engineering scaffolds, *Biomaterials*, 2017, **140**, 170–188, DOI: 10.1016/j.biomaterials.2017.06.005.
17 F. P. W. Melchels, J. Feijen and D. W. Grijpma, A review on stereolithography and its applications in biomedical engineering, *Biomaterials*, 2010, **31**(24), 6121–6130, DOI: 10.1016/j.biomaterials.2010.04.050.
18 N. Paunović, Y. Bao, F. B. Coulter, K. Masania, A. K. Geks, K. Klein, A. Rafsanjani, J. Cadalbert, P. W. Kronen and N. Kleger, *et al.*, Digital light 3D printing of customized bioresorbable airway stents with elastomeric properties, *Sci. Adv.*, 2021, **7**(6), eabe9499.
19 X. Kuang, J. Wu, K. Chen, Z. Zhao, Z. Ding, F. Hu, D. Fang and H. J. Qi, Grayscale digital light processing 3D printing for highly functionally graded materials, *Sci. Adv.*, 2019, **5**(5), eaav5790, DOI: 10.1126/sciadv.aav5790.
20 T. J. Wallin, J. H. Pikul, S. Bodkhe, B. N. Peele, B. C. Mac Murray, D. Therriault, B. W. McEnerney, R. P. Dillon, E. P. Giannelis and R. F. Shepherd, Click chemistry stereolithography for soft robots that self-heal, *J. Mater. Chem. B*, 2017, **5**(31), 6249–6255, DOI: 10.1039/C7TB01605K.
21 J. M. Sirrine, V. Meenakshisundaram, N. G. Moon, P. J. Scott, R. J. Mondschein, T. F. Weiseman, C. B. Williams and T. E. Long, Functional siloxanes with photo-activated, simultaneous chain extension and crosslinking for lithography-based 3D printing, *Polymer*, 2018, **152**, 25–34, DOI: 10.1016/j.polymer.2018.02.056.
22 C. J. Thrasher, J. J. Schwartz and A. J. Boydston, Modular Elastomer Photoresins for Digital Light Processing Additive Manufacturing, *ACS Appl. Mater. Interfaces*, 2017, **9**(45), 39708–39716, DOI: 10.1021/acsami.7b13909.
23 T. Zhao, R. Yu, S. Li, X. Li, Y. Zhang, X. Yang, X. Zhao, C. Wang, Z. Liu and R. Dou, *et al.*, Superstretchable and Processable Silicone Elastomers by Digital Light Processing 3D Printing, *ACS Appl. Mater. Interfaces*, 2019, **11**(15), 14391–14398, DOI: 10.1021/acsami.9b03156.
24 C. Tugui, M. Cazacu, D. M. Manoli, A. Stefan and M. Duduta, All-Silicone 3D Printing Technology: Toward Highly Elastic Dielectric Elastomers and Complex Structures, *ACS Appl. Polym. Mater.*, 2023, **5**(10), 7936–7946, DOI: 10.1021/acsapm.3c01190.
25 K. Du, J. Basuki, V. Glattauer, C. Mesnard, A. T. Nguyen, D. L. J. Alexander and T. C. Hughes, Digital Light Processing 3D Printing of PDMS-Based Soft and Elastic Materials with Tunable Mechanical Properties, *ACS Appl. Polym. Mater.*, 2021, **3**(6), 3049–3059, DOI: 10.1021/acsapm.1c00260.
26 M. Sandmeier, N. Paunović, R. Conti, L. Hofmann, J. Wang, Z. Luo, K. Masania, N. Wu, N. Kleger and F. B. Coulter, *et al.*, Solvent-Free Three-Dimensional Printing of Biodegradable Elastomers Using Liquid Macrophotoinitiators, *Macromolecules*, 2021, **54**(17), 7830–7839, DOI: 10.1021/acs.macromol.1c00856.
27 J. Zhou, X. Allonas, A. Ibrahim and X. Liu, Progress in the development of polymeric and multifunctional

photoinitiators, *Prog. Polym. Sci.*, 2019, **99**, 101165, DOI: 10.1016/j.progpolymsci.2019.101165.

28 D. Zhu; J. Zhang; J. Lalevée and P. Xiao, *3D Printing with Light, Chapter 1 Novel photoinitiating systems for 3D printing*. ed. Xiao, P. and Zhang, J., De Gruyter, 2021; pp. 1–48.

29 J. Wang, S. Stanic, A. A. Altun, M. Schwentenwein, K. Dietliker, L. Jin, J. Stampfl, S. Baudis, R. Liska and H. Grützmacher, A highly efficient waterborne photoinitiator for visible-light-induced three-dimensional printing of hydrogels, *Chem. Commun.*, 2018, **54**(8), 920–923, DOI: 10.1039/C7CC09313F.

30 A. Widera, R. Conti, A. Cosola, A. Fäh, D. Thöny, M. Sangermano, J. Levalois-Grützmacher and H. Grützmacher, ACTIVE-BAPO – a versatile transfer agent for photoactive bis(acyl)phosphane oxide units, *Chem. – Eur. J.*, 2023, **29**, e202203842, DOI: 10.1002/chem.202203842.

31 A. Cosola, M. Sangermano, D. Terenziani, R. Conti, M. Messori, H. Grützmacher, C. F. Pirri and A. Chiappone, DLP 3D – printing of shape memory polymers stabilized by thermoreversible hydrogen bonding interactions, *Appl. Mater. Today*, 2021, **23**, 101060, DOI: 10.1016/j.apmt.2021.101060.

32 A. Cosola, R. Conti, V. K. Rana, M. Sangermano, A. Chiappone, J. Levalois-Grützmacher and H. Grützmacher, Synthesis of γ-cyclodextrin substituted bis(acyl)phosphane oxide derivative (BAPO-γ-CyD) serving as multiple photoinitiator and cross-linking agent, *Chem. Commun.*, 2020, **56**(35), 4828–4831, DOI: 10.1039/D0CC01732A.

33 J. Wang, A. Chiappone, I. Roppolo, F. Shao, E. Fantino, M. Lorusso, D. Rentsch, K. Dietliker, C. F. Pirri and H. Grützmacher, All-in-One Cellulose Nanocrystals for 3D Printing of Nanocomposite Hydrogels, *Angew. Chem., Int. Ed.*, 2018, **57**(9), 2353–2356, DOI: 10.1002/anie.201710951 (acccessed 2023/11/25).

34 N. Paunović, J.-C. Leroux and Y. Bao, 3D printed elastomers with Sylgard-184-like mechanical properties and tuneable degradability, *Polym. Chem.*, 2022, **13**(16), 2271–2276, DOI: 10.1039/D2PY00113F.

35 N. Paunović, D. Meyer, A. Krivitsky, A. R. Studart, Y. Bao and J. C. Leroux, 4D printing of biodegradable elastomers with tailorable thermal response at physiological temperature, *J. Controlled Release*, 2023, **361**, 417–426, DOI: 10.1016/j.jconrel.2023.07.053.

36 G. Gonzales, A. Chiappone, K. Dietliker, C. F. Pirri and I. Roppolo, Fabrication and Functionalization of 3D Printed Polydimethylsiloxane-Based Microfluidic Devices Obtained through Digital Light Processing, *Adv. Mater. Technol.*, 2020, **5**, 2000374, DOI: 10.1002/admt.202000374.

37 S. Villata, M. Canta, D. Baruffaldi, A. Pavan, A. Chiappone, C. F. Pirri and I. Roppolo, 3D printable acrylate polydimethylsiloxane resins for cell culture and drug testing, *Biomater. Sci.*, 2023, **11**, 2950, DOI: 10.1039/d3bm00152k.

38 R. Conti, A. Widera, G. Müller, C. Fekete, D. Thöny, F. Eiler, Z. Benkö and H. Grützmacher, Organocatalyzed Phospha-Michael Addition: A Highly Efficient Synthesis of Customized Bis(acyl)phosphane Oxide Photoinitiators, *Chem. – Eur. J.*, 2023, **29**, e202202563, DOI: 10.1002/chem.202202563.

39 A. Kalinina, N. Strizhiver, N. Vasilenko, N. Perov, N. Demchenko and A. Muzafarov, Polycondensation of Diethoxydimethylsilane in Active Medium, *Silicon*, 2015, **7**, 95–106, DOI: 10.1007/s12633-014-9233-z.

40 J. A. Dicks and C. Wooland, Thiol-X Chemistry: A Skeleton Key Unlocking Advanced Polymers in Additive Manufacturing, *Macromol. Mater. Eng.*, 2025, **310**, 2400445, DOI: 10.1002/mame.202400445.

41 W. Ma, N. Wright and Y. Wang, Norbornene Dicarboximide: A Green Alternative for Thiol-Norbornene Photopolymers, *ACS Macro Lett.*, 2024, **13**, 915–920, DOI: 10.1021/acsmacrolett.4c00334.

42 M. I. Segal, A. J. Bahnick, N. G. Judge and M. L. Becker, Synthesis and Solvent Free DLP 3D Printing of Degradable Poly(Allyl Glycidyl Ether Succinate), *Angew. Chem.*, 2025, **64**, e202414016, DOI: 10.1002/ange.202414016.

43 N. Bhattacharjee, C. Parra-Cabrera, Y. T. Kim, A. P. Kuo and A. Folch, Desktop-Stereolithography 3D-Printing of a Poly(dimethylsiloxane)-Based Material with Sylgard-184 Properties, *Adv. Mater.*, 2018, **30**, 1800001, DOI: 10.1002/adma.201800001.

44 R. Xie, S. Mukherjee, A. E. Levi, V. G. Reynolds, H. Wang, M. L. Chabinyc and C. M. Bates, Room temperature 3D printing of super-soft and solvent-free elastomers, *Sci. Adv.*, 2020, **6**, eabc6900, DOI: 10.1126/sciadv.abc6900.

45 M. Vtankhah-Varnosfaderani, W. F. M. Daniel, M. H. Everhart, A. A. Pandya, H. Liang, K. Matyjaszewski, A. V. Dobrynin and S. S. Sheiko, Mimicking biological stress–strain behaviour with synthetic elastomers, *Nature*, 2017, **549**, 497–501, DOI: 10.1038/nature23673.

46 K. K. Nikoo, J. R. Brwon, G. Nayyar, T. E. Long and J. L. Self, Vat Photopolymerization of Supersoft Acrylamide-Based PDMS Bottlebrush Elastomers, *ACS Appl. Polym. Mater.*, 2025, **7**, 9234–9242, DOI: 10.1021/acsapm.5c01527.